JOURNAL OF PROPULSION AND POWER
Vol. 16, No. 6, November–December 2000

Starting Envelope of the Subdetonative Ram Accelerator

E. Schultz,* C. Knowlen,† and A. P. Bruckner‡
University of Washington, Seattle, Washington 98195

An experimental investigation has been undertaken to explore the effects of propellant composition, entrance Mach number, and projectile throat area variation on the subdetonative ram accelerator starting process. Upper and lower limits on these parameters provide bounding conditions under which a supersonic projectile can successfully initiate and stabilize the combustion-supported shock system on the projectile necessary for acceleration. Relatively energetic propellant combined with high entrance Mach number are observed to push the shock system ahead of the projectile, whereas low energy release together with low entrance Mach number are conducive to the shock system falling behind. Decreasing entrance Mach number also causes the shock system to propagate ahead of the projectile under some circumstances, suggesting that fundamentally different start failure mechanisms are responsible. Increasing the flow area at the throat lowers the Mach number for choking the diffuser, but causes difficulty in containing the combustion-supported shock system unless the Mach number is increased or the propellant energy release is decreased. Trends observed in this investigation and prior research are used to develop a generalized starting envelope, illustrating where the success and failure boundaries lie in relation to one another on the propellant energy release vs Mach number plane.

Introduction

THE ram accelerator is a hypervelocity launcher in which a projectile, similar in shape to the centerbody of a ramjet, travels supersonically through a tube filled with premixed gaseous fuel and oxidizer (Fig. 1).[1,2] The ideal starting process begins with a conventional gun accelerating the projectile and obturator from rest through an evacuated launch tube (Fig. 2).[3] A diaphragm separates the launch tube from the high-pressure, propellant-filled ram accelerator tube (Fig. 3a). The projectile pierces the diaphragm and enters the propellant at a supersonic entrance Mach number. The propellant is compressed on the conical projectile nose up to the projectile throat and expands over the body where it encounters the obturator (Fig. 3b). A normal shock is driven onto the projectile body as the obturator separates from the projectile and rapidly decelerates (Fig. 3c). The propellant energy is released in a combustion zone behind the normal shock, thermally choking the flow behind the projectile. The choked flow stabilizes the normal shock on the projectile body, creating a high-pressure zone at its base that results in sustained acceleration of the projectile through the tube (Fig. 3d). The starting process is loosely defined as the period of time between projectile acceleration from rest to the point where the flowfield illustrated in Fig. 1 is stabilized.

Development of a robust starting process is instrumental for utilizing the ram accelerator in a variety of applications. Summaries of past research on numerous factors influencing the starting process at the University of Washington and other ram accelerator facilities are presented by Schultz et al.[3] and Schultz.[4] Recent investigations of the role that the obturator plays together with start failures caused by propellant detonation are reported in Ref. 5. The research presented here explores the effect of entrance Mach number, propellant composition, and projectile throat area on the starting process at entrance Mach numbers lower than the Chapman–Jouguet (CJ) detonation Mach number. Envelopes of operating conditions under which successful starts occur are derived from the experimental results, and a generalized starting envelope is developed based on trends observed while varying the aforementioned parameters.

Experimental Procedure

The experiments were conducted in the 38-mm-bore University of Washington (UW) ram accelerator facility (Fig. 2).[6] It consists of a light-gas gun initial launcher with a 6-m launch tube, a launch tube dump tank, 16 m of ram acceleration tube, a final dump tank, and a catcher tube. There are two instrument stations in the launch tube, 12 and 139 mm before the entrance diaphragm. The first instrument station in the ram accelerator tube is located 12 mm after the diaphragm, followed by a station 227 mm from the diaphragm. There is a 400-mm interval between subsequent stations in the remainder of the ram accelerator tube. All stations were instrumented with electromagnetic sensors and piezoelectric pressure transducers (PCB 119) at the tube wall. Electromagnetic sensors provided a time-distance history of the projectile by detecting the passage of a magnet ($\pm 1\mu$s) located in the projectile throat. Differencing these data points resulted in velocity data with an uncertainty of approximately 1% based on the 1-μs diagnostic resolution, distance between instrument stations, and entrance velocities around 1200 m/s. The pressure transducers measured the flowfield pressure at the tube wall.

The initial launcher is a helium-filled, double-diaphragm, single-stage light-gas gun with a maximum pressurization capability of 40 MPa. The entrance Mach number to the ram accelerator test section is varied by adjusting the helium pressure to change the projectile/obturator velocity history in the launch tube and through propellant chemistry changes to adjust the acoustic speed. A 305-mm-long section of the launch tube beginning 0.6 m ahead of the entrance diaphragm has 36 holes, each of 6.4-mm diameter, through which gases in the launch tube are vented to an evacuated dump tank.[7] The nominal launch tube residual air pressure is 3–5 torr, monitored by a piezoresistive transducer (Kistler 4043A1). The entrance diaphragms are made of Mylar, up to 0.72 mm thick for a 5-MPa fill pressure.

The propellant characteristics are tailored by the type and concentration of fuel, oxidizer, and diluent used in the mixture. A propellant class is characterized by its fuel–oxygen stoichiometry and the variable concentration of a specific diluent. The nominal UW starting process propellant for the entrance velocity range of 1100–1200 m/s is $2.8CH_4 + 2O_2 + 5.7N_2$ at a 2.5–5 MPa fill pressure, with small variations in the methane and nitrogen content. The gas handling system is based on sonic orifice metering and is supported by gas chromatography. Absolute mixture accuracy is within 5%, and the

Received 15 May 1999; revision received 16 September 1999; accepted for publication 18 September 1999. Copyright © 1999 by the authors. Published by the American Institute of Aeronautics and Astronautics, Inc., with permission.

*Graduate Research Assistant, Department of Aeronautics and Astronautics; currently at the California Institute of Technology, Pasadena, CA. Student Member AIAA.

†Research Scientist, Department of Aeronautics and Astronautics. Senior Member AIAA.

‡Professor and Department Chair, Department of Aeronautics and Astronautics. Fellow AIAA.

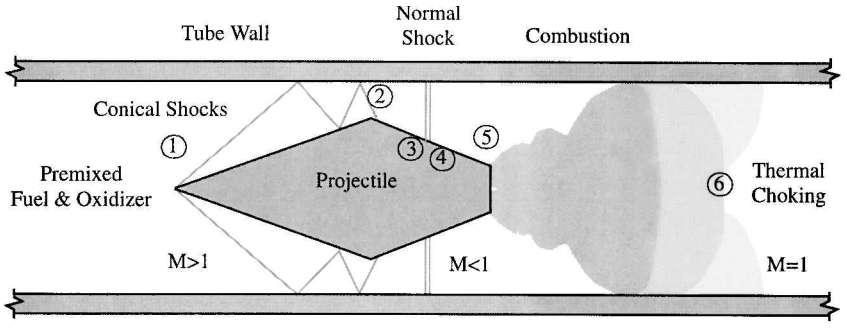

Fig. 1 Ram accelerator propulsive mechanism at subdetonative velocities with quasi-one-dimensional model station numbers.

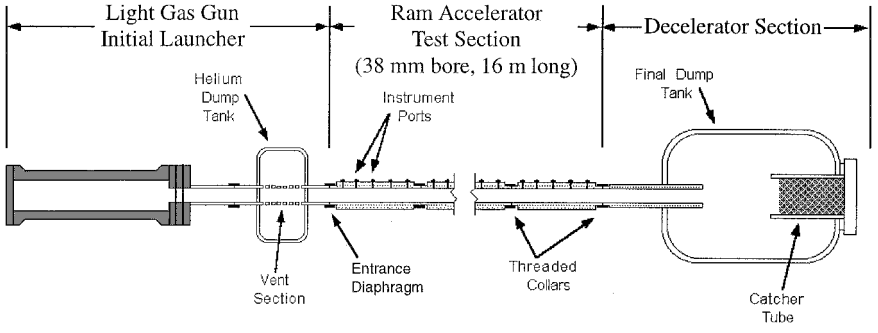

Fig. 2 Ram accelerator facility schematic.

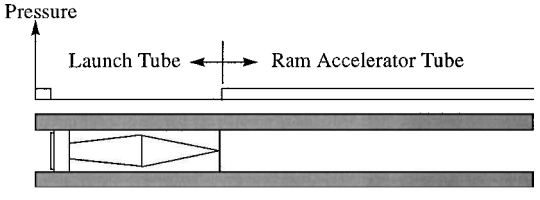

a) Projectile and obturator just prior to entrance diaphragm

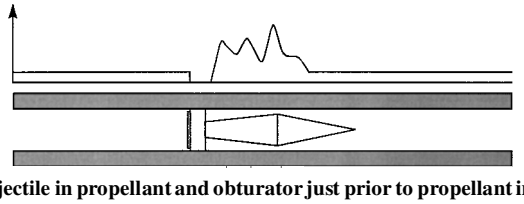

b) Projectile in propellant and obturator just prior to propellant impact

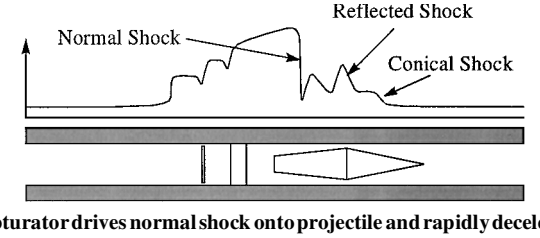

c) Obturator drives normal shock onto projectile and rapidly decelerates

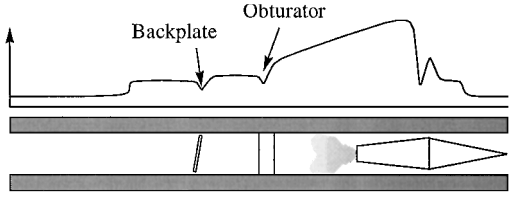

d) Combustion zone stabilizes normal shock on projectile body

Fig. 3 Primary features of successful starting process.

relative precision when varying mixtures is within 1%. Propellant properties of interest include the acoustic speed and the energy release parameter $Q = \Delta q / c_p T$, where the equilibrium energy release Δq is normalized by the constant pressure specific heat capacity c_p and the temperature T of the undisturbed mixture. The energy release parameter is often taken at the CJ state, in which case $Q = Q_{CJ}$. Chemical reactions rates, induction lengths, and activation energies, collectively referred to as reactivity parameters, are also of interest but difficult to quantify under typical ram accelerator operating conditions.

The ram accelerator projectile shown in Fig. 4 is typically fabricated of 7075-T6 aluminum alloy and consists of two pieces, the nose and body, which thread together at the throat. Primary characteristics of this projectile include a 10-deg half-angle nose, 4.5-deg taper from throat to base, a flow-throat-to-tube area ratio (A_{throat}/A_{tube}) of 0.42, a flow-base-to-tube area ratio of 0.64 (including fins), and a mass of approximately 75 g. Projectiles with four and five fins having these primary characteristics (the fins of four-finned projectiles are 25% thicker than those of five-finned projectiles to provide similar flow occlusion) demonstrate the same behavior during the starting process and will henceforth be referred to as standard projectiles. Specifications of these and the other projectiles used in this investigation are provided in Table 1. Increasing the projectile throat diameter while maintaining constant base area results in scaled-up projectiles having reduced flow-throat-to-tube area ratios and longer body lengths than the standard projectiles.[8] Projectiles having larger than standard A_{throat}/A_{tube} and the same body length and taper angle were used in investigations of throat area variation (TAV) projectiles. Increasing the body taper angle while keeping the throat and base areas constant results in a short projectile.[9] A magnet located in the throat allows tracking of the projectile with the electromagnetic sensors.

The 38.1-mm-diam (±0.05-mm) polycarbonate obturator (Fig. 4), comprises a solid backplate (3 g) glued to a perforated cylinder (13 g), prevents blow-by of the initial launcher gas, and assists propellant ignition in the ram accelerator tube. In some experiments a magnet was epoxied into a circumferential groove in the perforated cylinder to facilitate tracking the obturator. Experiments conducted with combustible mixtures are referred to as hot shots (HS), whereas those in noncombustible mixtures are referred to as cold shots (CS).

Table 1 Projectile configurations

Type	No. of fins	A_{throat}/A_{tube}	Fin width, mm	Nose angle, deg	Body length, mm	Body taper, deg	Mass, g
Scaled-up	4	0.25	3.8	10	94.7	4.5	85
	4	0.29	3.8	10	88.9	4.5	77
	4	0.34	3.8	10	82.6	4.5	73
	4	0.38	3.8	10	76.2	4.5	65
Standard	4	0.42	3.8	10	71.1	4.5	75
	5	0.42	3.0	10	71.1	4.5	76
Short	4	0.42	3.8	15	46.0	6.9	50
TAV 1	3	0.42	3.8	10	71.1	4.5	69
TAV 2	3	0.50	3.8	10	71.1	4.5	72
TAV 3	3	0.59	3.8	10	71.1	4.5	62

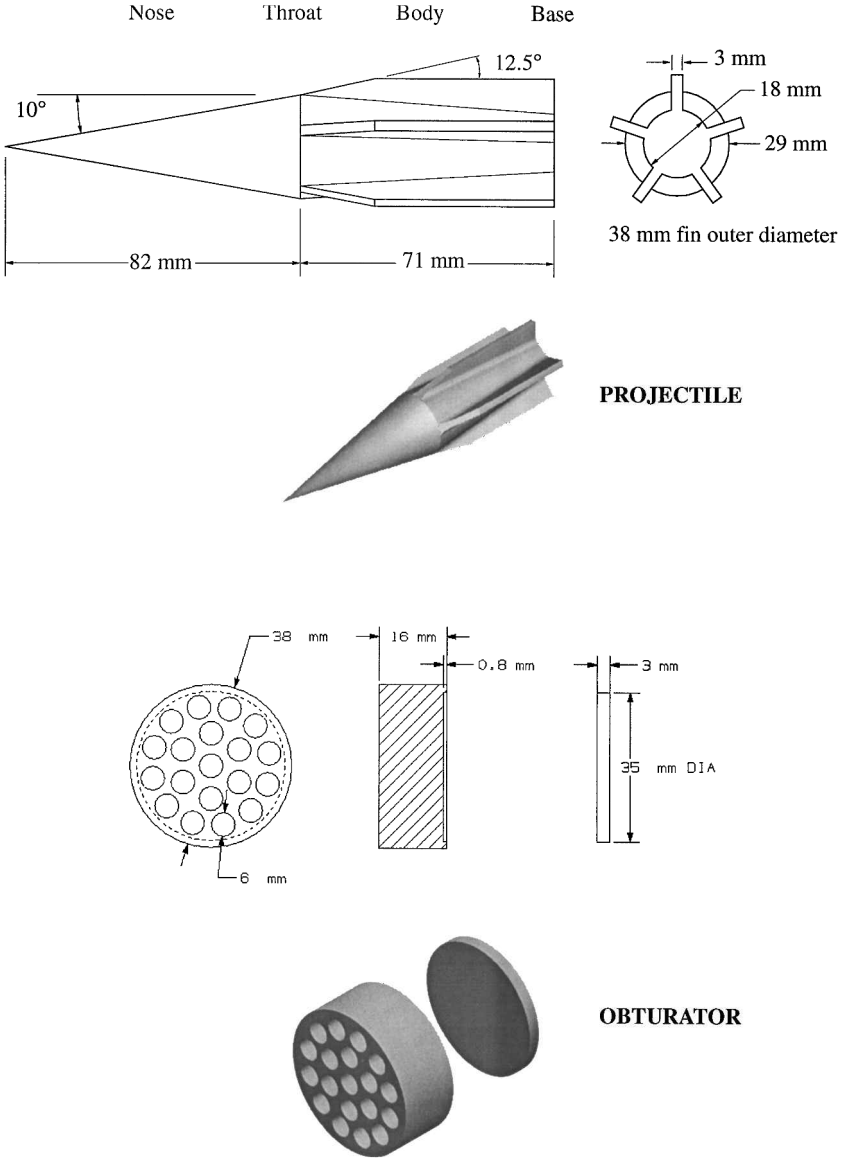

Fig. 4 Standard ram accelerator projectile and obturator.

The result of a start attempt was discerned from the projectile velocity profile and the tube wall pressure data. Any experiment in which the projectile accelerated for more than 2 m (1.7-ms time-of-flight in propellant at 1200-m/s entrance velocity) was deemed a successful start. Experiments in which the projectile did not accelerate for at least 2 m were considered start failures and identified as a sonic diffuser unstart, wave unstart, or wave fall-off, based on analysis of the tube wall pressure data as discussed in Ref. 3 and summarized in the following section.

Possible Start Attempt Outcomes

Experiments have identified four possible outcomes of a start attempt[3]: successful start, sonic diffuser unstart, wave fall-off, and wave unstart. A successful start (Fig. 5a) is achieved when supersonic flow is maintained throughout the diffuser and the normal shock system is stabilized on the projectile body through propellant energy release. Plots of a projectile velocity distance and tube wall pressure data for a successful ram accelerator start are presented in Fig. 6. The location of the entrance diaphragm is at 0 m. The tube

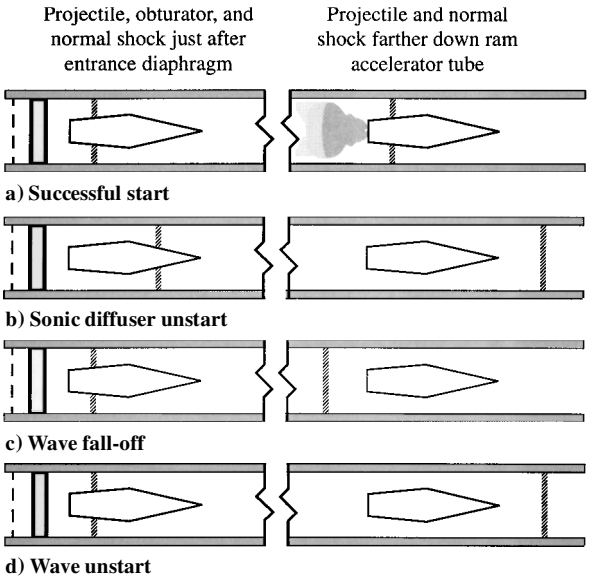

Fig. 5 Possible outcomes of an attempted start.

wall pressure data, presented as measured pressure normalized by propellant fill pressure, are shown as a series of traces that originate from different instrumentation stations along the tube. A projectile outline is shown scaled relative to the average velocity. The conical shock from the projectile nose tip is evident as the first pressure rise. The next shock impacts the tube wall in the projectile throat region and is followed by a pressure drop arising from the subsequent flow expansion. The following shock is assumed to be the leading wave of the combustion-supported normal shock system. Reflected oblique shocks, appearing as periodic pressure fluctuations in the traces from the other instrument stations, extend into the full tube area behind the projectile.[10] The pressure trace from the station at 1427 mm shows the tail of the signal decaying below the fill pressure due to thermal drifting of the piezoelectric pressure transducer. Erosion of the thermal protection material varies for individual transducers, and so not all transducers exhibit this phenomenon. On successful starting, the projectile velocity steadily increases at a rate consistent with that predicted for the thermally choked propulsive mode.[11]

A sonic diffuser unstart (Fig. 5b) is caused by conditions upstream of the throat resulting in choked flow at the projectile throat. Compression waves emanating from the sonic region coalesce into a shock that propagates ahead of the projectile, causing rapid deceleration. Figure 7 shows a projectile velocity profile and tube wall

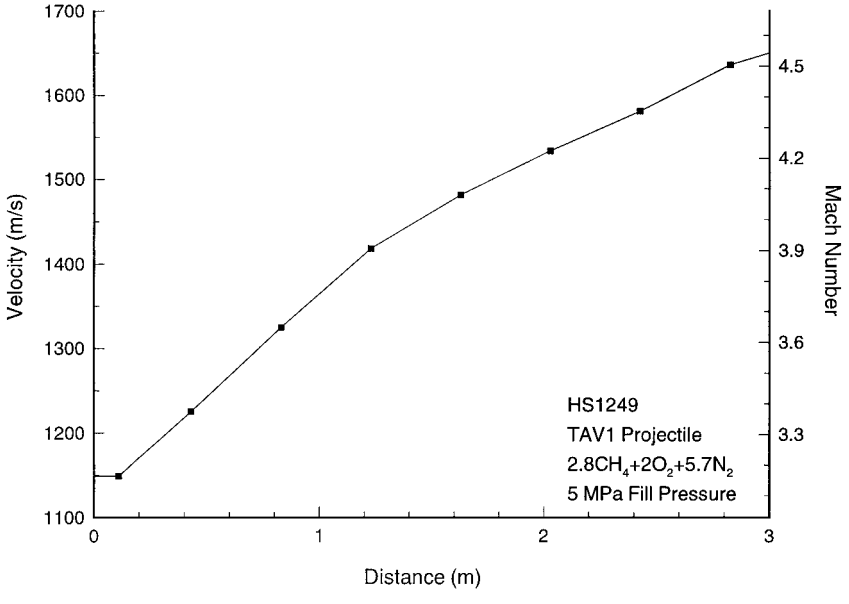

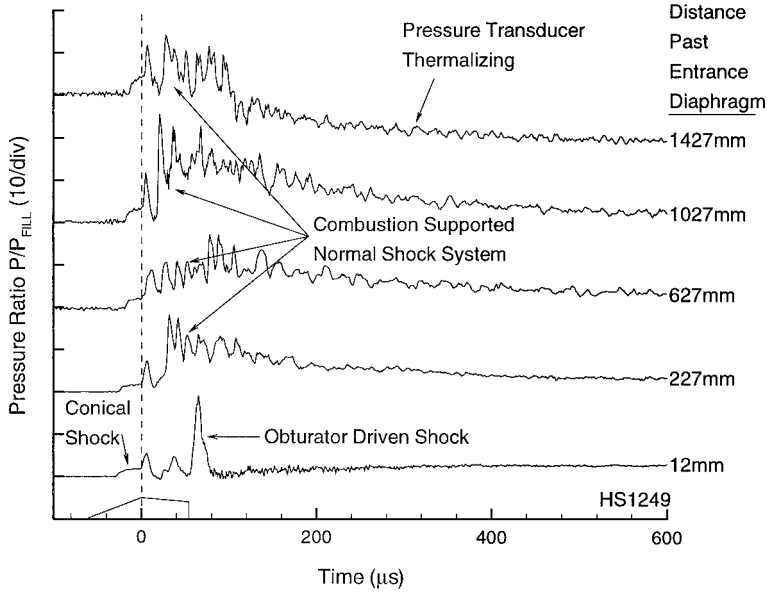

Fig. 6 Experiment resulting in a successful start.

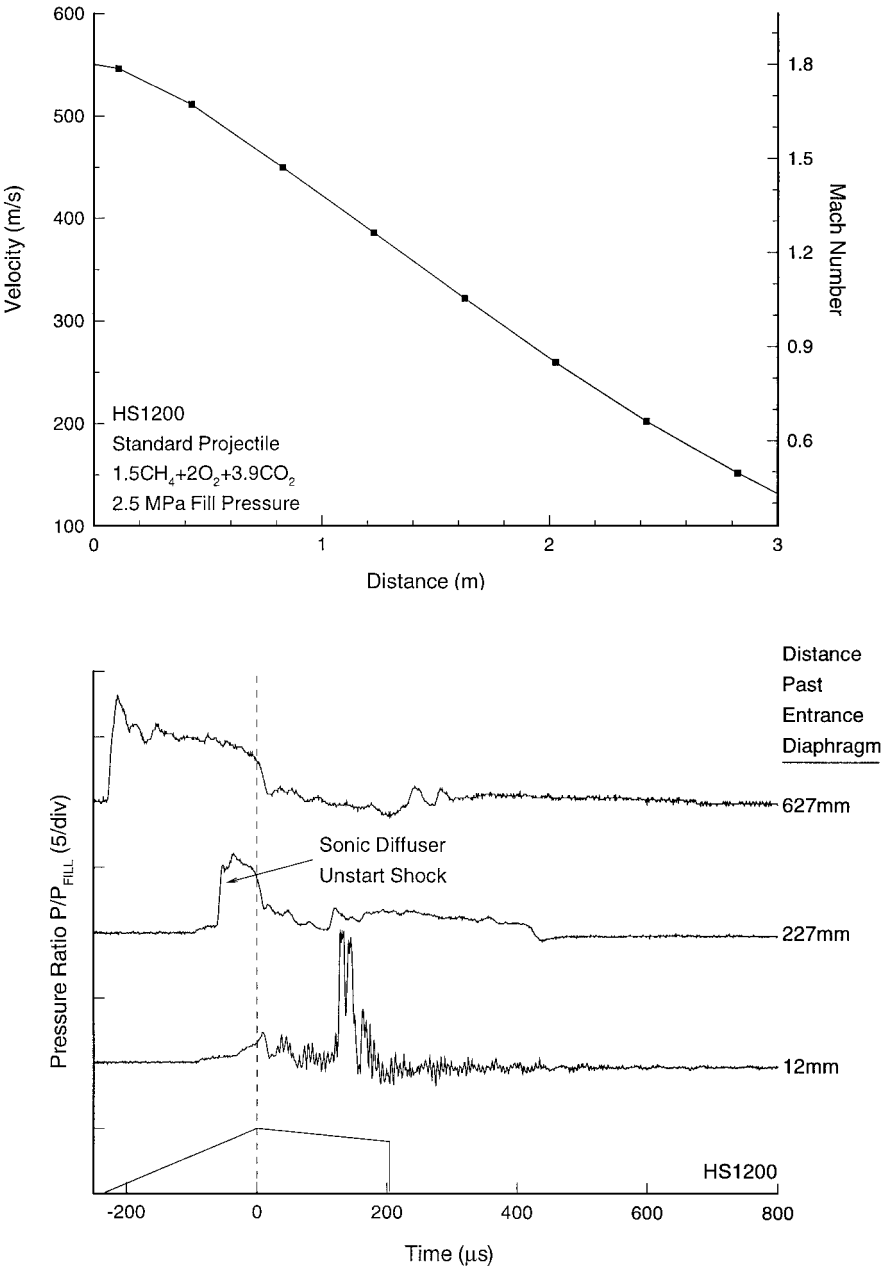

Fig. 7 Experiment resulting in a sonic diffuser unstart.

pressure data from a shot that resulted in a sonic diffuser unstart caused by a low entrance Mach number. The projectile velocity steadily decreases following entry into the ram accelerator tube, and the pressure trace 227 mm past the entrance diaphragm shows the shock that arises after the sonic diffuser unstart. The spatial separation between the first two pressure traces past the entrance diaphragm does not permit detailed observation of the unstart shock wave formation.

A wave fall-off (Fig. 5c) occurs when insufficient energy is released from the propellant to keep the normal shock system on the projectile body from receding behind the base. The projectile outruns this shock system and decelerates due to supersonic drag as it travels through the tube. Figure 8 exhibits a projectile velocity profile and tube wall pressure data from a wave fall-off experiment. The velocity increases after projectile entry due to the high base pressure generated by the obturator, and then decreases after the obturator-supportedshock system recedes from the projectile body. The experiment eventually resulted in a sonic diffuser unstart after the projectile was sufficiently decelerated. The wave fall-off data presented in Fig. 8 have the same features as the data collected when a projectile enters a nonreactive mixture.[3]

A wave unstart (Fig. 5d) is caused by conditions behind the throat resulting in disgorgment of the shock system into the diffuser. The projectile then rapidly decelerates in the high-pressure region behind the shock. Projectile velocity vs distance and tube wall pressure data from a shot in which the unstart wave developed in the projectile wake are presented in Fig. 9. A high-amplitude shock in the projectile wake is first observed 1027 mm past the entrance diaphragm, and it can be seen to have surged beyond the projectile throat by the 1427-mm location. In other wave unstart cases, the high-amplitude shock appears to form first on the projectile body and sometimes not as a discrete shock, but rather as a broad, high-pressure region originating in the wake or on the body. These significant variations in pressure history data observed during wave unstarts suggest that there exists more than one wave unstart mechanism.[3,6]

Experimental Results

The effects of entrance Mach number M, propellant energy release Q, and projectile throat area on the starting process are discussed hereafter. The experimental data are presented on plots in the Q–M plane and indicate whether a successful start, sonic diffuser

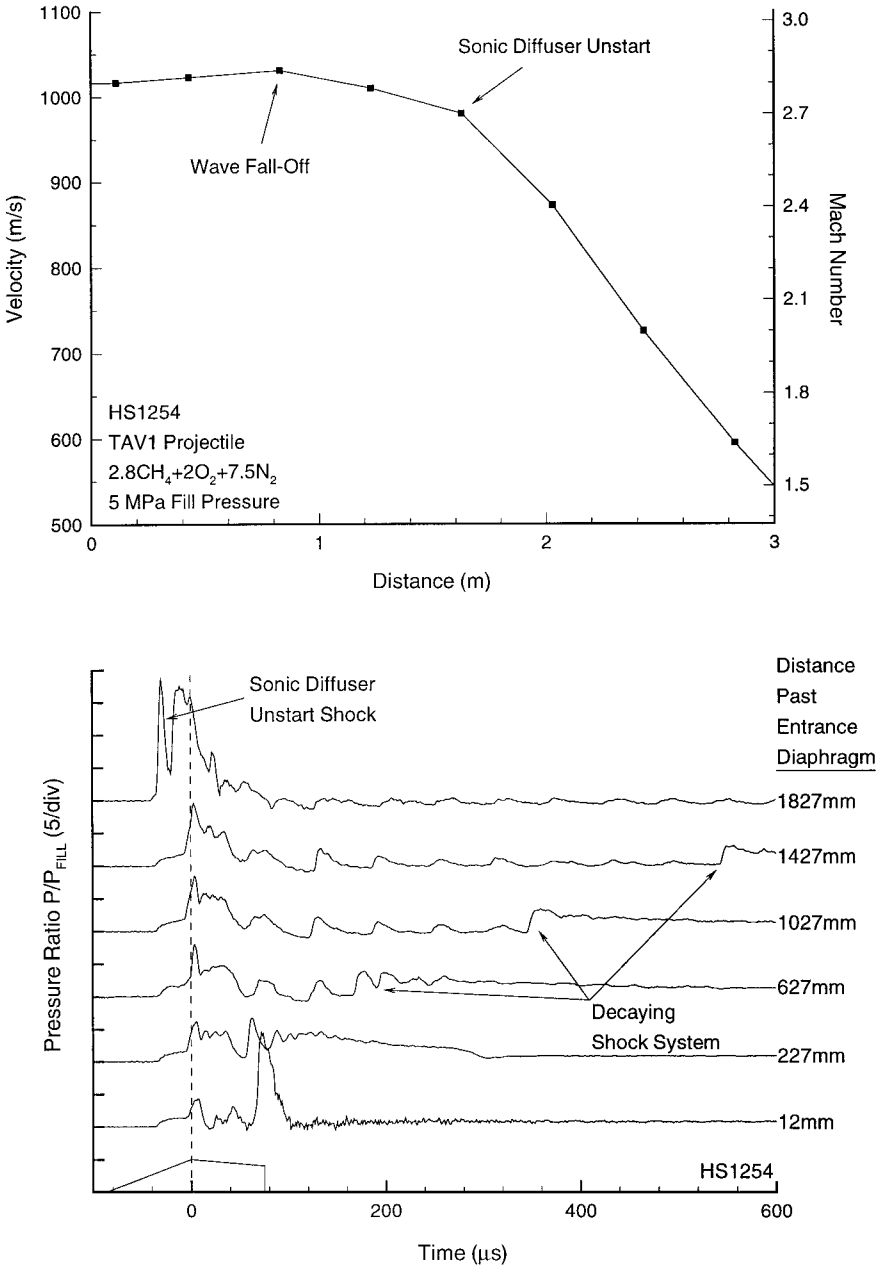

Fig. 8 Experiment resulting in a wave fall-off.

unstart, wave fall-off, or wave unstart occurred. The large amount of data presented eliminates the possibility of discussion of each individual data point. Instead, trends and other salient features are brought to attention for use in later analysis.

Mach Number and Energy Release

The results of 518 start attempts using standard and TAV1 projectiles at fill pressures ranging from 2–5 MPa in a propellant composition range of $2.8CH_4 + 2O_2 + (4.5\text{–}7.5)N_2$ are presented in Fig. 10. Experiments conducted with an entrance Mach number of 2.8 showed that a 5% reduction in energy release changed the outcome from a wave unstart to a wave fall-off. An increase of entrance Mach number from 2.8 to 2.9 in the propellant having $Q_{CJ} = 4.6$ changed the result from a wave unstart to a successful start, thus indicating a lower bound on entrance Mach number to the starting of this projectile. No upper bound on entrance Mach number has yet been found under these experimental conditions. Successful starting of the ram accelerator was achieved with energy release parameters ranging from $4.4 < Q_{CJ} < 5.3$. Because of as yet unexplained reasons, an occasional wave fall-off and wave unstart were observed within this regime of the Q–M plane, giving a 94% reliability of starting under these conditions.

Results of attempts to start a standard projectile in 2.5 MPa $CH_4/O_2/CO_2$ propellants between Mach 2.5 and 2.9 are presented in Fig. 11. When Q was gradually increased by reducing CO_2 dilution in experiments conducted at a particular entrance Mach number, the results changed abruptly from a wave fall-off to a wave unstart. The Q level at which this change in start outcome occurs was found to increase as the entrance Mach number was decreased. There were no successful starts for this particular propellant class at these values of M, even though Q was varied in such small increments that carbon dioxide concentrations were changed by only 0.1 mole at a time.

The results of 32 start attempts at 5 MPa with a short projectile (Table 1) are presented in Fig. 12 for fuel-rich CH_4/O_2 and CH_4/O_2/He propellants.[9] Variations in methane were used to adjust the Q of these propellants while the entrance velocity was kept constant (1325 ± 15 m/s). Successful starts were achieved in the range $5.0 < Q_{CJ} < 5.3$ at an entrance Mach number of ~ 3.3 in CH_4/O_2,

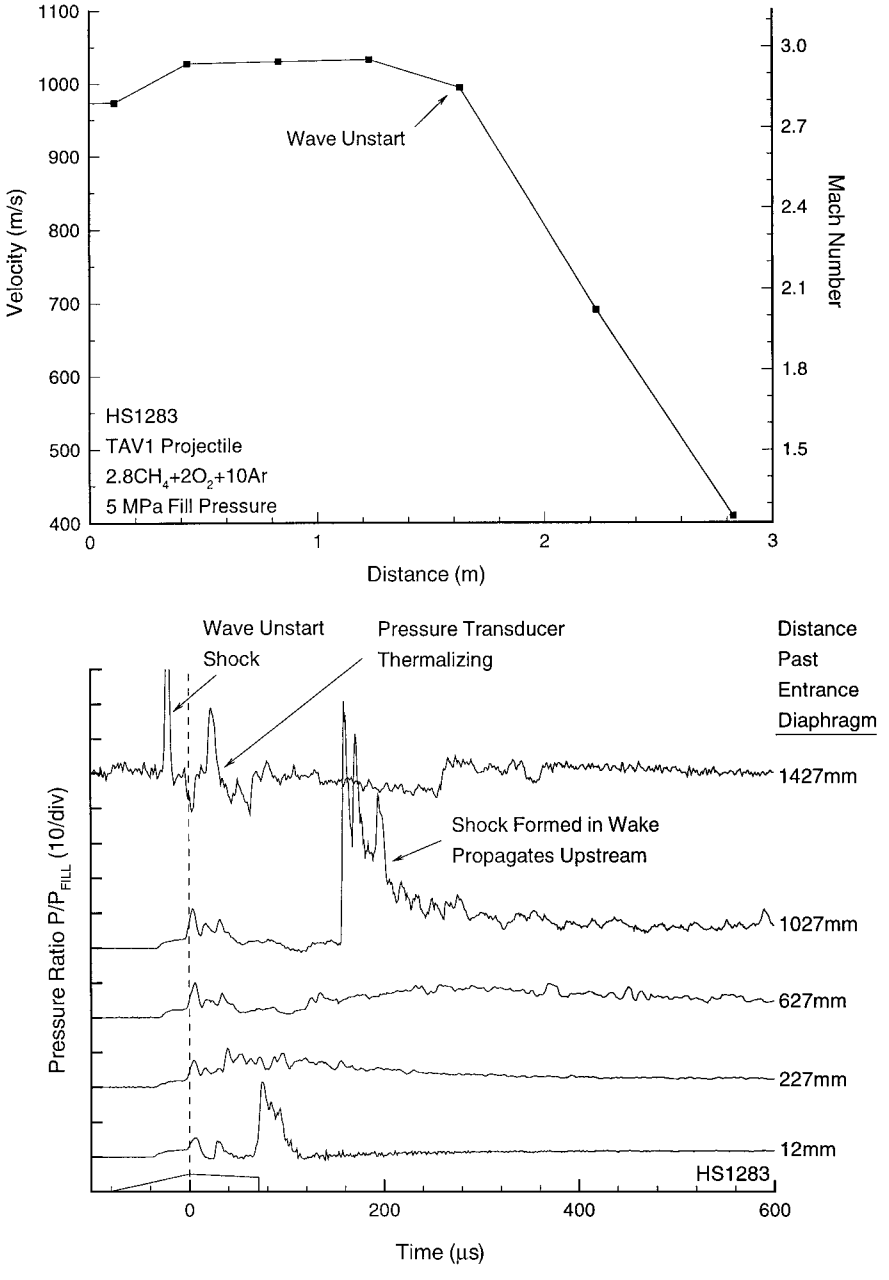

Fig. 9 Experiment resulting in a wave unstart.

and more energetic propellants resulted in wave unstarts. Adding 2 moles of helium to the methane-rich propellant reduced the entrance Mach number to approximately 3. Under these conditions Q had to be reduced to 4.8 before a successful start could be achieved.

The results of start attempts with the TAV projectiles in 5-MPa argon- and nitrogen-diluted propellants are presented in Figs. 13 and 14, respectively. All three TAV projectile geometries (Table 1) exhibited the same trends stated earlier, which are summarized as follows:

1) Relatively low Q and M are conducive to a wave fall-off result. A wave fall-off will occur in the limit of a nonreactive propellant ($Q = 0$) at Mach numbers above the sonic diffuser unstart limit, M_{sdu}, and, therefore, relatively low propellant energy release is expected to have the same result. Under conditions of decreasing M there exists a lower limit at which the propellant cannot be ignited, irrespective of Q.

2) Relatively high Q leads to wave unstarts. Excessive energy release behind a projectile pushes the shock system ahead of the throat. Wave unstarts also occur at higher and lower M than those that permit a successful start. These phenomena, observed on either side of the successful start regime, suggest multiple mechanisms for producing a wave unstart.[3,6] A projectile at low M may be ill suited for containing the combustion wave, whereas a high entrance Mach number might be conducive to directly initiating a detonation or releasing energy in the immediate vicinity of the throat.

Note that Q is a parameter that cannot be used for comparisons among different propellant classes. In other words, a particular methane, oxygen, and nitrogen propellant will, in general, not exhibit the same starting characteristics as a methane, oxygen, and argon mixture that has the same value of Q. Energy release is quantified by Q, but does not take the other reactive characteristics of a propellant into account. A supporting example is provided by two TAV3 start attempts at approximately Mach 3.5 in $Q_{CJ} = 4.0$ propellants at a 5-MPa fill pressure, one in $2.8CH_4 + 2O_2 + 10.1Ar$ and the other in $2.8CH_4 + 2O_2 + 8N_2$. With all other conditions held the same, the argon-diluted experiment resulted in a wave unstart with detonation within 0.5 m of entrance, whereas the nitrogen-diluted experiment resulted in a successful start (Figs. 13 and 14, respectively).

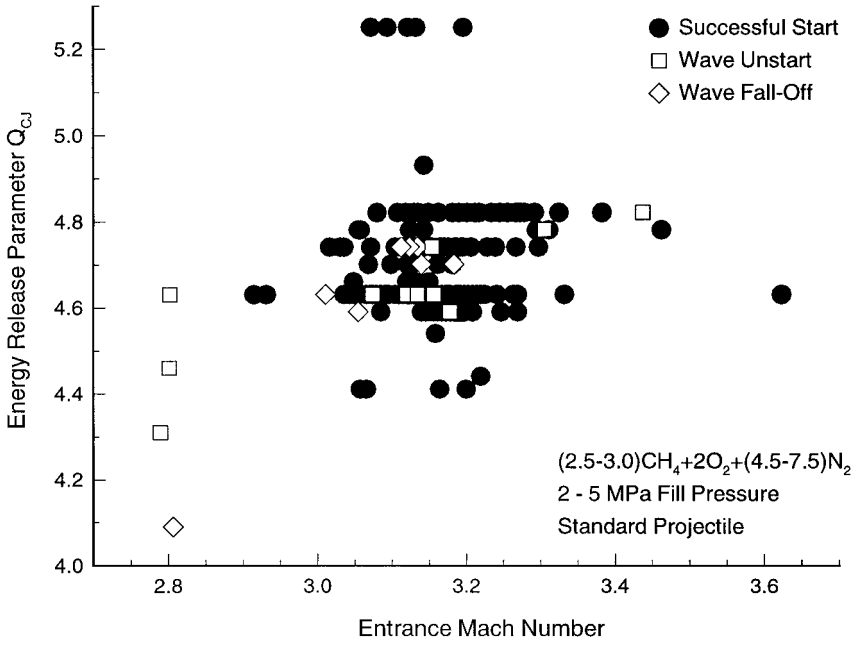

Fig. 10 Start attempt results with the standard projectile in nitrogen-diluted propellant.

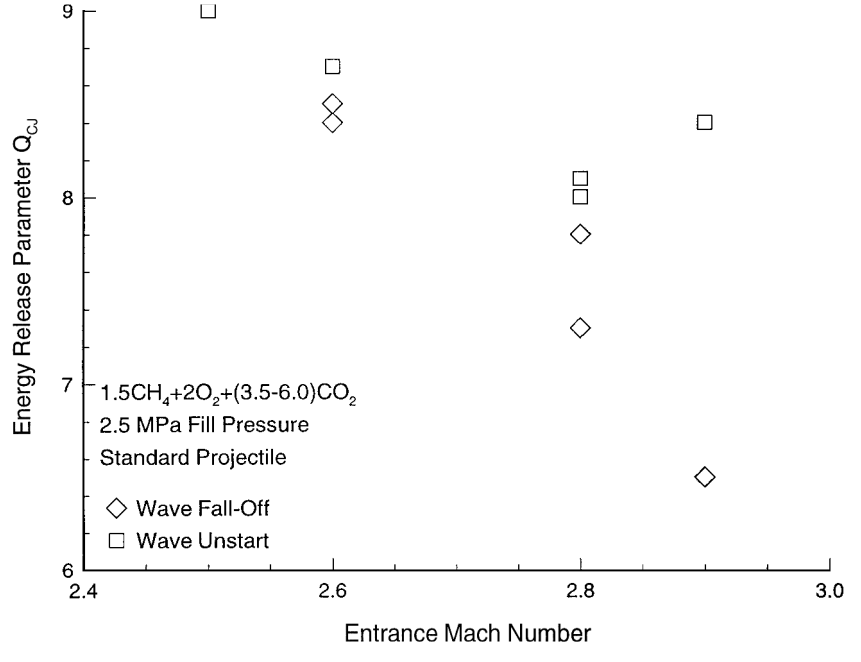

Fig. 11 Start attempt results with the standard projectile in carbon dioxide-diluted propellant.

Throat Area

Figure 13 contains highlighted data points at particular Q and M conditions for which a TAV1 projectile experiences a wave fall-off where a TAV2 successfully starts, as well as another Q–M condition at which a TAV2 wave fall-off corresponds to a wave unstart result for a TAV3. Figure 14 illustrates a Q–M condition resulting in a TAV2 successful start and a TAV3 wave unstart. The complete body of data from Figs. 13 and 14 indicates that, for a fixed Q and M, projectiles with increased flow area at the throat tend to disgorge the shock system that can be contained by projectiles having less throat flow area. Increased throat flow areas require reduced Q and/or increased M to contain the shock system. Only the TAV2 projectile was successfully started in the argon-diluted propellants (Fig. 13). All three TAV configurations were successfully started in nitrogen-diluted propellants, although under different Q–M conditions (Fig. 14). Successful starts were achieved by increasing M and decreasing Q as the throat flow area increased.

Start attempt results for 193 projectiles of varying throat area in the nominal $2.8CH_4 + 2O_2 + 5.7N_2$ propellant at pressures in the range of 2–5 MPa are presented in Fig. 15. The nominal throat flow area ratio ($A_{\text{throat}}/A_{\text{tube}} = 0.42$) was able to successfully start from Mach 2.9 to 3.6. Successful starts occurred for several throat flow area ratios below 0.42, illustrating that a reduced throat flow area can contain the normal shock system in this propellant as long as the diffuser flow is supersonic. The problem that arises with very small throat flow areas is the increased M for sonic diffuser unstart. An experiment with a 0.25 throat flow area ratio projectile resulted in a sonic diffuser unstart at Mach 3.24, whereas higher throat flow areas permitted a successful start at this value of M. When the throat flow area ratio was increased to 0.50, wave unstarts resulted at a value

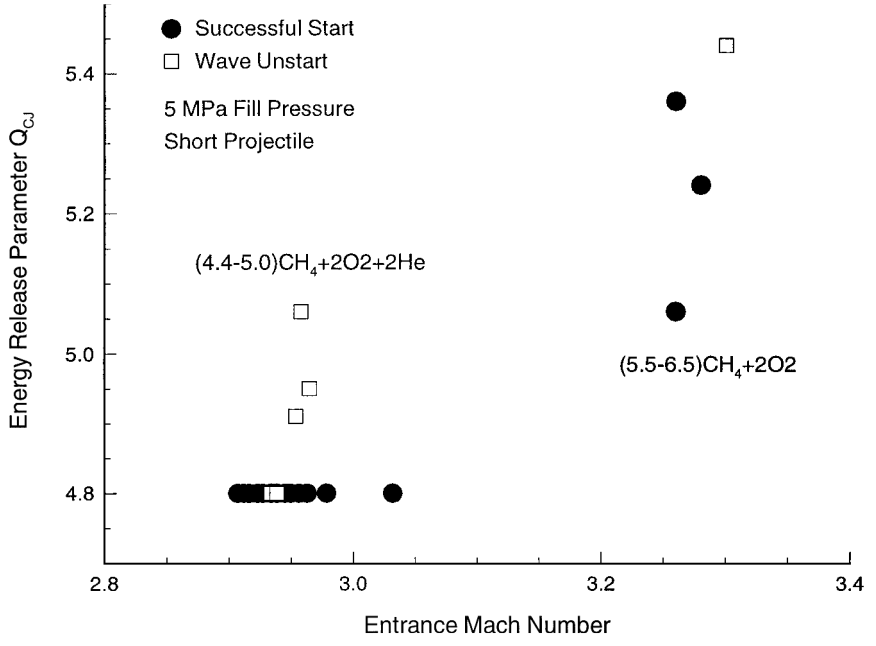

Fig. 12 Start attempt results with the short projectile in methane/oxygen and methane/oxygen/helium propellants.

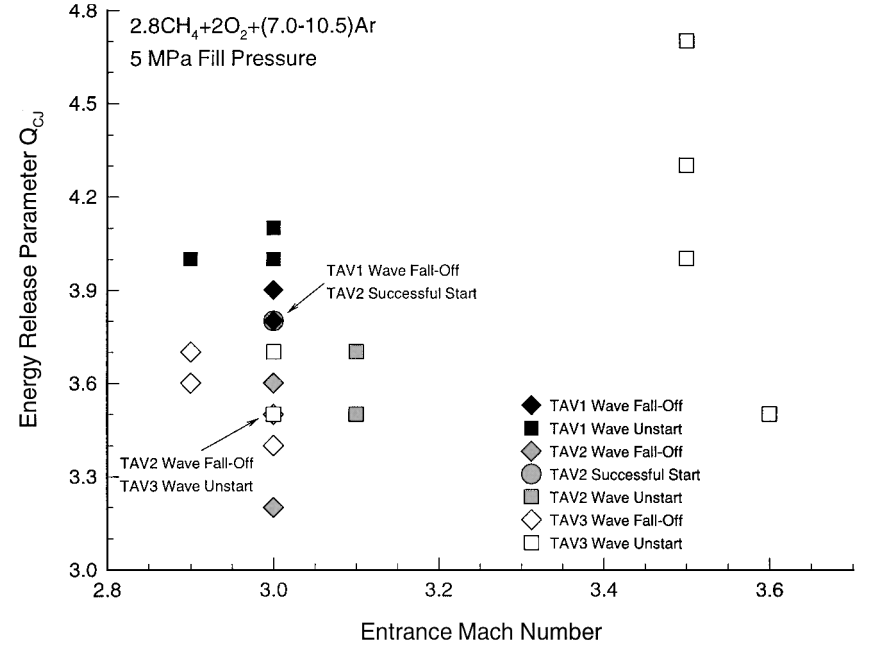

Fig. 13 Start attempt results with throat area variation projectiles in argon-diluted propellant.

of M, where successful starts were observed for the nominal area ratio. Greater throat flow area seems conducive to disgorgment of the shock system under Q and M conditions in which a smaller throat flow area can contain the shock system.

Experimentally determined sonic diffuser unstart Mach numbers M_{sdu} for the TAV projectiles in 5-MPa, $CH_4/O_2/Ar$ propellants are plotted in Fig. 16, along with the projectile Mach number necessary for steady supersonic flow through a diffuser as given by the area-Mach number relation,[12]

$$\frac{A_{\text{tube}}}{A_{\text{throat}}} = \left(\frac{P_{02}}{P_{01}}\right)\frac{1}{M_{\text{sdu}}}\left[\frac{2}{\gamma+1}\left(1+\frac{\gamma-1}{2}M_{\text{sdu}}^2\right)\right]^{(\gamma+1)/2(\gamma-1)}$$

where P_{02}/P_{01} is the total pressure ratio of the conical diffuser. The theoretical M_{sdu} for several diffuser total pressure ratios is also plotted in Fig. 16. It can be seen that the diffuser total pressure loss at M_{sdu} decreases with increasing flow area, which is a consequence of lower M, less nose cone surface area, and alterations in the shock train structure between the tube wall and conical nose. The data are taken from wave fall-off shots in which the projectile decelerated due to drag until the diffuser could no longer remain supersonic. Initially obtaining supersonic flow through the diffuser is a different gasdynamic process from choking an already supersonic diffuser,[12] and, therefore, the value of M_{sdu} required for successful diffuser starting on entrance is expected to be different from the Mach number limit measured for projectile diffusers that successfully start followed by drag deceleration to a diffuser unstart.

Note that in all throat flow area variation experiments (Figs. 13–16), the throat area was not the only projectile geometry variable changed. The base diameter was reduced as the throat diameter was reduced to maintain a constant body taper angle for the TAV projectiles. The reduced throat flow area experiments with scaled-up

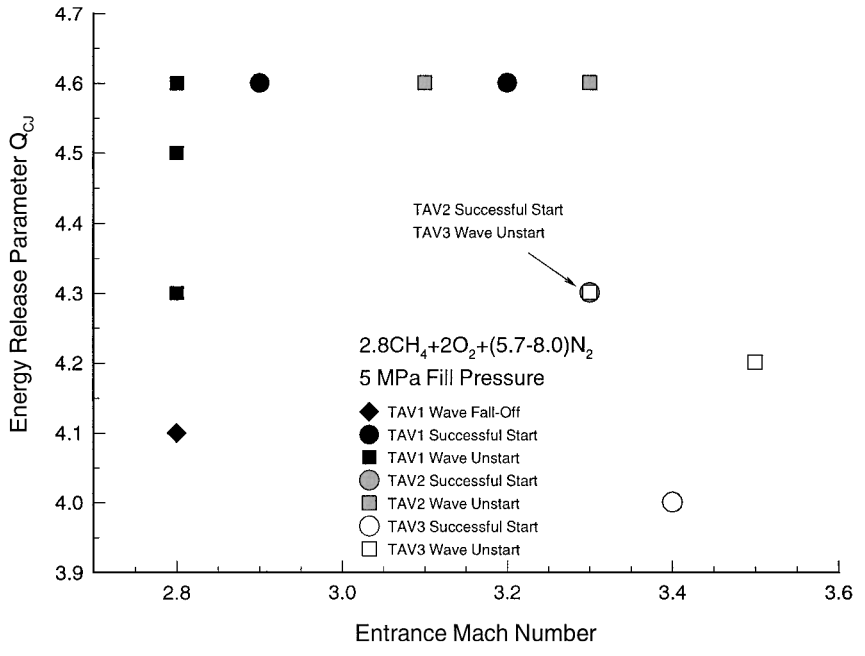

Fig. 14 Start attempt results with throat area variation projectiles in nitrogen-diluted propellant.

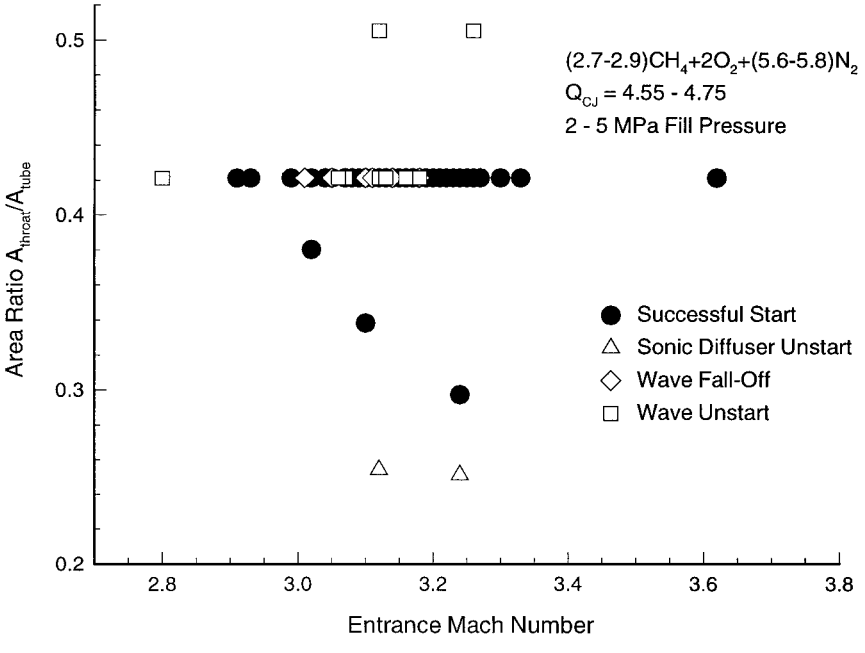

Fig. 15 Start attempt results with varying throat flow area in nitrogen-diluted propellants.

projectiles (Fig. 15) incorporated changes in body length, rather than base diameter, to provide a constant taper angle as the throat diameter varied. Therefore, the results presented in this section cannot be attributed to a variation in only the throat area without a more detailed parametric investigation.

Analysis

In the following sections, the results presented earlier are compared to a quasi-one-dimensional model of the ram accelerator that predicts operational limits and are used to construct a generalized starting envelope.

Quasi-One-Dimensional Model

Station numbers for a quasi-one-dimensional model of the thermally choked ram accelerator that predicts an operational envelope are presented in Fig. 1 (Ref. 13). Global assumptions of this model include inviscid steady flow of a calorically perfect gas. Quasi-one-dimensional isentropic flow analysis is employed between stations 1 and 2, 2 and 3, and 4 and 5. The influence of nonisentropic phenomena on the flowfield is ignored for this discussion because they do not qualitatively affect the results.[13] Normal shock jump conditions are used between stations 3 and 4, and heat addition resulting in thermal choking is assumed to occur at full tube area between stations 5 and 6. Given a projectile Mach number, this model produces three limits to ram accelerator operation: choked flow between stations 1 and 2 (sonic diffuser unstart), energy release for which the normal shock is located at a flow area ratio greater than that at the projectile base (wave fall-off), and energy release for which the normal shock is located at a flow area ratio smaller than that at the projectile throat (wave unstart). These limits represent the three start failures, and, therefore, it is useful to compare experimental

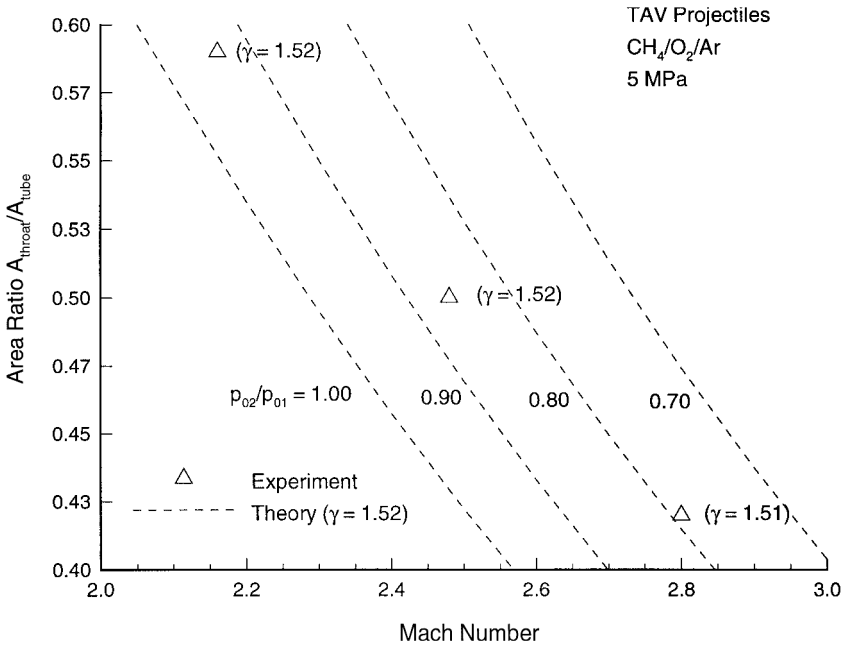

Fig. 16 Experimental vs theoretical comparison of the sonic diffuser unstart Mach number.

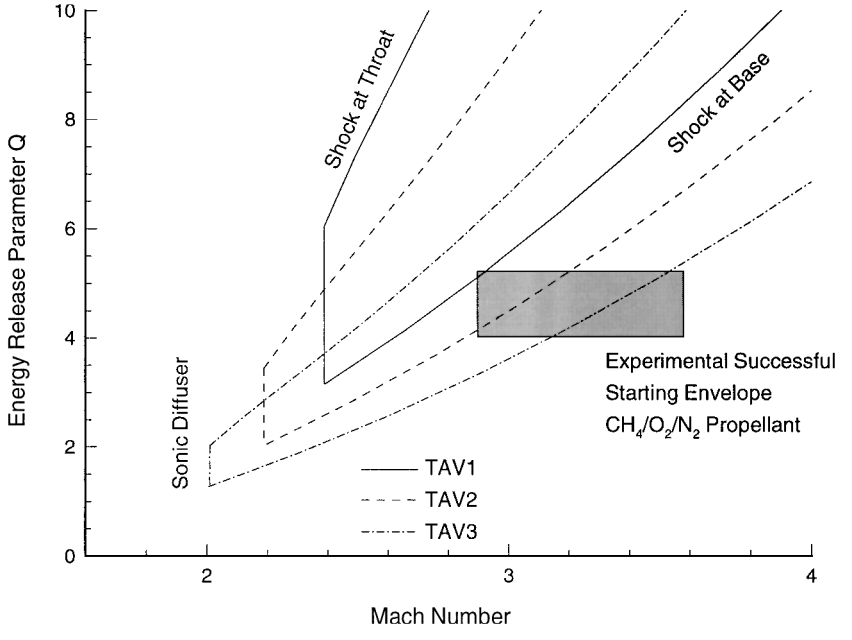

Fig. 17 Limits of operation predicted by the quasi-one-dimensional model for three different throat area ratios and the experimental successful starting envelope.

start attempt data with the envelope of operation predicted by this model.

The predicted operational envelopes for the projectiles used in this investigation are presented in Fig. 17 along with the experimentally determined envelope for successful starting in $CH_4/O_2/N_2$ propellants. The presence of the perforated obturator during the starting process will influence the range of Q and M in which the ram accelerator can be operated; however, the qualitative effects of variable Q, M, and throat and base area ratios predicted by this theoretical model are still relevant. There is a Mach number limit below which the flow will choke ahead of the throat, resulting in a sonic diffuser unstart. Above this Mach number, low Q tends to cause a wave fall-off whereas high Q results in a wave unstart. Increasing flow area at the throat shifts the sonic diffuser unstart limit to a lower Mach number. Reduced throat flow area allows operation with higher Q at a given M than projectiles having the nominal flow throat area. Reducing the base area of the projectile lowers the Q at which a wave fall-off is predicted to occur and increases the theoretical maximum operational Mach number.

The experimentally observed successful starting envelope (M = 2.9–3.6 and Q = 4.0–5.3) lies almost entirely outside of the model envelope, below the shock at base limit (Fig. 17). This finding is not surprising given the simplistic, steady-state nature of the model. Many factors relevant to the starting process are unaccounted for, including the presence of an obturator, residual launch tube gas, and propellant reactive characteristics.[3–5] For example, the obturator acts to overdrive the normal shock prior to thermal choking and thereby would shift the shock at throat and shock at base model limits downward. Future analytical modeling efforts on the starting process will incorporate such effects.

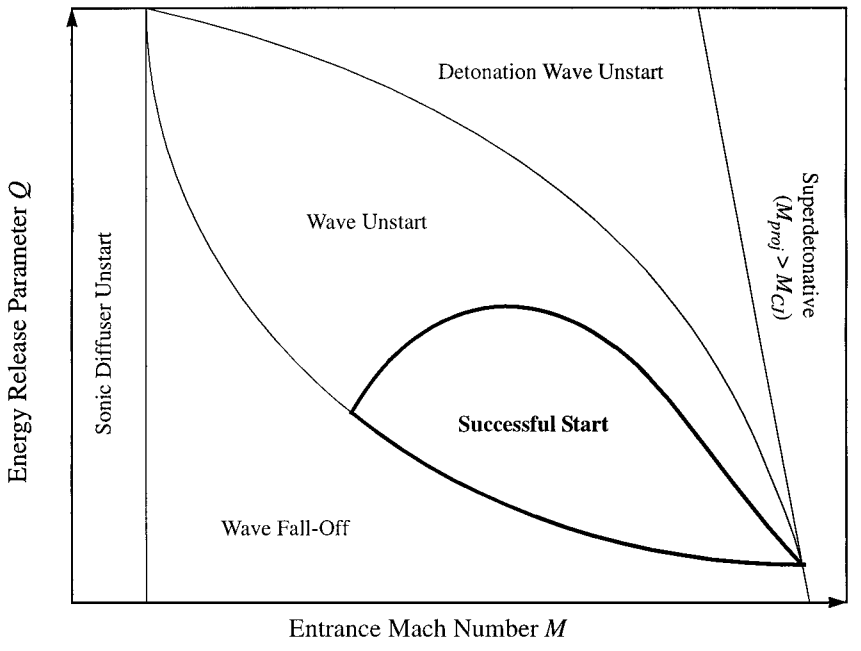

Fig. 18 Generalized starting envelope.

Generalized Starting Envelope

For a given projectile, obturator, and other initial conditions, it is desirable to obtain a starting envelope that illustrates the dependence on the propellant chemistry and entrance Mach number. Theoretical and computational analyses of the ram accelerator to date are inadequate for accurately determining such a starting envelope. The lack of a sufficiently comprehensive parametric experimental study to identify chemistry and Mach number regimes conducive to successful starting precludes the presentation of a quantitative starting envelope as well. However, based on the present experimental investigation of the starting process and that presented in Ref. 6, a qualitative starting envelope can be constructed. This generalized starting envelope in the Q–M plane is presented in Fig. 18 with axes values left off to underscore its qualitative nature.

The following comments summarize the experimental and analytical observations made in this study that have been used to construct the limits drawn on the Q–M plane. A sonic diffuser unstart occurs at M less than M_{sdu} where supersonic flow to the projectile throat cannot be maintained. The CJ detonation Mach number M_{CJ}, which has a modest dependence on Q (varying as $Q^{1/2}$), sets an upper limit on starting in the subdetonative velocity regime. The wave fall-off phenomenon dominates the region of relatively low Q and M where the propellant cannot be ignited or release enough energy to keep the shock system on the projectile body. A detonation wave unstart region, in which the projectile and obturator initiate a detonation immediately on entrance, exists for relatively high Q and M (Ref. 6). Other types of wave unstarts, caused by yet undetermined mechanisms, have been observed to occur at constant Q when M is 1) increased from a wave falloff result, 2) decreased from a detonation wave unstart result, or 3) decreased from a successful start result. Wave unstarts have also been observed to occur at constant M when Q is 1) increased from a wave falloff result, 2) decreased from a detonation wave unstart result, or 3) increased from a successful start result. The successful start envelope is then bounded by the aforementioned start failure modes.

Care should be exercised to realize that any quantitative Q–M plane starting envelope will only be applicable to a particular set of initial conditions including projectile and obturator characteristics, propellant class, launch tube conditions, etc. Furthermore, recall that Q is a parameter that cannot be used for comparison across mixture classes. With all other conditions held the same, equal Q propellants from different classes have been shown to result in different start outcomes. An improved propellant correlating parameter for the starting process other than Q would greatly simplify data presentation and understanding but is likely to be very complex, given the various reactive characteristics of each propellant mixture.

The starting process is so complex in sheer number of factors involved and so rich in phenomena that computational fluid dynamics (CFD) holds considerable potential for studying the starting process as an adjunct to extensive parametric experimental investigations. However, the challenges confronting the application of CFD are many: unsteady, three-dimensional, mixed subsonic and supersonic regions; shock waves; turbulent and separated flows; and chemical kinetics in a variety of propellants at pressures high enough to make real gas effects important. High-resolution experimental data for CFD validation could ultimately provide a complete understanding of the starting process and, therefore, quantitative prediction of successful starting limits.

Conclusions

Propellant composition, entrance Mach number, and projectile throat area were found to have significant effects on the starting process of a ram accelerator projectile, leading to all of the possible outcomes: successful start, sonic diffuser unstart, wave fall-off, and wave unstart. The present results are qualitatively supported by the limits to operation predicted by a quasi-one-dimensional ram accelerator model, but quantitative agreement is poor. Relatively energetic propellants are observed to lead to wave unstarts, whereas decreasing energy release is conducive to wave fall-off. Wave unstarts occur at Mach numbers lower and higher than those resulting in a successful start, lending support to the theory that multiple mechanisms may be responsible for causing a wave unstart. Relatively low Mach numbers lead to wave fall-offs until the sonic diffuser unstart limit is reached. Increasing flow area at the throat lowers the sonic diffuser unstart limit, but has a tendency to disgorge the combustion-supported shock system, resulting in wave unstarts unless the entrance Mach number is increased or the propellant energy release is decreased. Trends observed during the experimental investigation of the parameters listed earlier were used to develop a generalized starting envelope on the Q–M plane. This envelope details where the possible start outcome regimes lie in relation to one another, providing a guide to help establish new ram accelerator facilities and develop more robust starting processes in existing launch systems.

Acknowledgment

The effort presented here was supported by Army Research Office Grant DAAL03-92-G-0100.

References

[1]Hertzberg, A., Bruckner, A. P., and Bogdanoff, D. W., "Ram Accelerator: A New Chemical Method for Accelerating Projectiles to Ultrahigh Velocities," *AIAA Journal*, Vol. 26, No. 2, 1988, pp. 195–203.

[2]Bruckner, A. P., Knowlen, C., Hertzberg, A., and Bogdanoff, D. W., "Operational Characteristics of the Thermally Choked Ram Accelerator," *Journal of Propulsion and Power*, Vol. 7, No. 5, 1991, pp. 828–836.

[3]Schultz, E., Knowlen, C., and Bruckner, A. P., "Overview of the Subdetonative Ram Accelerator Starting Process," *Ram Accelerators*, edited by K. Takayama and A. Sasoh, Springer–Verlag, Berlin, 1998, pp. 189–203.

[4]Schultz, E., "The Subdetonative Ram Accelerator Starting Process," M.S. Thesis, Dept. of Aeronautics and Astronautics, Univ. of Washington, Seattle, WA, 1997.

[5]Schultz, E., Knowlen, C., and Bruckner, A. P., "Obturator and Detonation Experiments in the Subdetonative Ram Accelerator," *Shock Waves*, Vol. 9, No. 3, 1999, pp. 181–191.

[6]Bruckner, A. P., Burnham, E. A., Knowlen, C., Hertzberg, A., and Bogdanoff, D. W., "Initiation of Combustion in the Thermally Choked Ram Accelerator," *Shock Waves*, edited by K. Takayama, Springer–Verlag, Berlin, 1992, pp. 623–630.

[7]Stewart, J. F., Bruckner, A. P., and Knowlen, C., "Effects of Launch Tube Shock Dynamics on Initiation of Ram Accelerator Operation," *Ram Accelerators*, edited by K. Takayama and A. Sasoh, Springer–Verlag, Berlin, 1998, pp. 181–188.

[8]Imrich, T. S., "The Impact of Projectile Geometry on Ram Accelerator Performance," M.S. Thesis, Dept. of Aeronautics and Astronautics, Univ. of Washington, Seattle, WA, 1995.

[9]Elvander, J. E., Knowlen, C., and Bruckner, A. P., "High Acceleration Experiments Using a Multi-Stage Ram Accelerator," *Ram Accelerators*, edited by K. Takayama and A. Sasoh, Springer–Verlag, Berlin, 1998, pp. 55–64.

[10]Hinkey, J. B., Burnham, E. A., and Bruckner, A. P., "High Spatial Resolution Measurements of Ram Accelerator Gas Dynamic Phenomena," AIAA Paper 92-3244, 1992.

[11]Knowlen, C., "Theoretical and Experimental Investigation of the Thermodynamics of the Thermally Choked Ram Accelerator," Ph.D. Dissertation, Dept. of Aeronautics and Astronautics, Univ. of Washington, Seattle, WA, April 1991.

[12]Oates, G. C., *Aerothermodynamics of Gas Turbine and Rocket Propulsion*, AIAA Education Series, AIAA, Washington DC, 1988, pp. 206–210.

[13]Higgins, A. J., Knowlen, C., and Bruckner, A. P., "Ram Accelerator Operating Limits Part 1: Identification of Limits," *Journal of Propulsion and Power*, Vol. 14, No. 6, 1998, pp. 951–958.